Effects of Micro-polar Fluids and the Tsann Roughness Model on Performance Characteristics of Two-lobe Bearings

Rohollah Shafaei[1], Mohammad Hadi Shafaei[2]

[1] *Mr., Engineering Department, Yazd University, Yazd, Iran*
[2] *Mr., Engineering Department, Shiraz University, Shiraz, Iran*

ABSTRACT

In the lubrication theories, the bearing surfaces are generally considered as smooth and without any roughness but actually these are not accurate. In order to find the bearing performance parameters it is required to solve the lubrication equation. Without necessary simplifications, solving such equation is terribly difficult. By adding the roughness effects to the problem, the necessity of using numerical methods become more obvious.
The surface irregularities play an important role in the bearing mechanical behaviors. Such roughness, cause conversion in lubricated film thickness that effect on lubrication parameters. The considered fluids in this investigation were incompressible micro polar fluids that contain ingredients, which will endure the physical stresses and moments.
In this article, using the finite element method, the effects of surface roughness on the lubrication of two-lobe bearings performance were proposed. Roughness numerical modeling was approached by the Tsann method. At first, the computer program had been written for the smooth case and then the program was developed for the bearings with roughness on their surfaces. The problem was resolved for two different surface profiles and the results were compared. The results indicate that considering the thickness of lubricant layer with the Tsann roughness theory will increase the pressure distribution and load carrying capacity but it reduce the coefficient of friction and side leakage flow.

Keyword: *surface roughness, Tsann method, finite element, micro polar fluids, two-lobe bearings*

1. Introduction

So far, different models have been presented for roughness. For example, it can be said one-dimensional finite element model for hydrodynamic bearing [1]. In this study, both the longitudinal and transverse roughness are modeled. Fluid film thickness was applied as a random variable, and the issue has been studied in stable condition. He changed the Reynolds equation based on defined parameters to modeling a roughness problem [2].
Prasad examined the performance of a circular bearing that was affected by temperature changes and the rough three-dimensional roughness [3]. Ferro fluids performance evaluated in round short bearing considering roughness [4]. The results show increasing the loading capacity and reducing the coefficient of friction.
The first research of non-circular bearings was been done by Pinkus [5] which presented a load capacity and energy losses in two-lobe bearings. Then, Lund and Thomsen [6] obtained the non-circular bearing performance parameters with the finite difference method. Their report is one of the most available resources to design non-circular bearings in which various geometrical parameters were been noted that affect the performance of this bearings.
Recently, regarding this subject, the FEM [7] and GDQ [8] numerical methods have been used to solve the equations without considering roughness.

The surface roughness was been investigated by taking Tsann hypothesis and using the finite element method in this paper. By substituting in the governing equations, the lubricant film thickness is expressed in terms of Tsann functions to achieve pressure distributions and the lubricant performance parameters of two-lobe bearings.

2. Mathematical formulation of the problem

Generally, Navier-Stokes equations include statements: inertia, pressure, mass, and viscosity which solving such equations is a complex analytical work. In a series of issues, pressure and viscosity are the only prominent parameters which their flow are called slow viscous motion and the fluid layer problems are categorized in this group. Therefore, the modified and non-dimensional Reynolds equation of bearings for micro polar lubricants is as follows [7]:

$$\frac{\partial}{\partial\theta}\left(\bar{\Psi}\left(N,l_m,\bar{h}\right)\frac{\partial\bar{p}}{\partial\theta}\right)+\frac{R^2}{L^2}\frac{\partial}{\partial\bar{z}}\left(\bar{\Psi}\left(N,l_m,\bar{h}\right)\frac{\partial\bar{p}}{\partial\bar{z}}\right)=6\frac{\partial\bar{h}}{\partial\theta} \tag{1}$$

In which:

$$\bar{\Psi}\left(N,l_m,\bar{h}\right)=\bar{h}^3+12\frac{\bar{h}}{l_m^{\,2}}-6N\,\frac{\bar{h}^2}{l_m}Coth\left(\frac{N\,l_m\,\bar{h}}{2}\right)$$

$$l_m=\frac{C}{\Lambda},\quad \Lambda=\left(\frac{C_a+C_d}{4\mu}\right)^{\frac{1}{2}},\quad N=\left(\frac{\mu_r}{\mu+\mu_r}\right)^{\frac{1}{2}}$$

Dimensionless thickness of fluid film ($\bar{h}$) on the clearance between the shaft and two-lobe bearings is obtained via geometrical relationships in term of θ (fig 1).

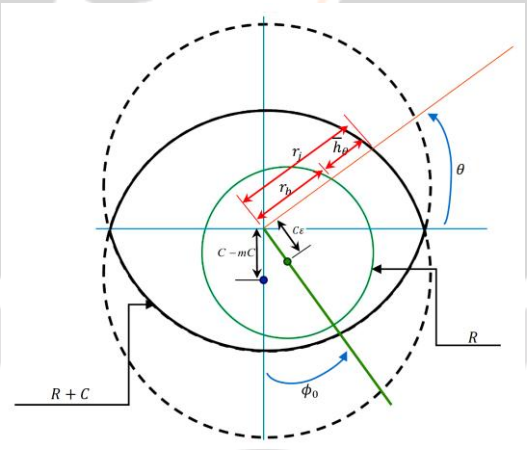

Fig 1: Lubricant film thickness in two-lobe bearing

Tsann Lin roughness method only affects lubricant film thickness. However, major changes will affect the nature of governing equation due to the adding of new independent variable in calculating the thickness of the lubricant film equations.

The lubricant film thickness is been calculated as follows [2]:

$$\bar{H}=\bar{h}+\bar{\delta} \tag{2}$$

$\bar{H}$ depicts the lubricant film thickness with roughness, $\bar{h}$ describes the lubricant film thickness without roughness and $\bar{\delta}$ is used as asperity profile.

By substituting $\bar{H}$ for $\bar{h}$, the governing equation is modified as follows:

$$\frac{\partial}{\partial\theta}\left(\bar{\Psi}\left(N,l_m,\bar{H}\right)\frac{\partial\bar{p}}{\partial\theta}\right)+\frac{R^2}{L^2}\frac{\partial}{\partial\bar{z}}\left(\bar{\Psi}\left(N,l_m,\bar{H}\right)\frac{\partial\bar{p}}{\partial\bar{z}}\right)=6\frac{\partial\bar{H}}{\partial\theta} \tag{3}$$

In which

$$\bar{\Psi}\left(N,l_m,\bar{H}\right)=\bar{H}^3+12\frac{\bar{H}}{l_m^{\,2}}-6N\frac{\bar{H}^2}{l_m}Coth\left(\frac{N\,l_m\bar{H}}{2}\right)$$

Both of θ and $\bar{z}$ directions have cosine curve in Tsann asperity profile. The geometric size of the asperity is defined by the height, $\bar{H}_a$, and the half width both in the θ direction, L_θ, and in the $\bar{z}$ direction, $L_{\bar{z}}$. The asperity profile is expressed mathematically as

$$\bar{\delta}\left(\theta,\bar{z}\right)=\frac{\bar{H}_a}{4}\left\{1+\cos\left[\frac{\pi}{L_\theta}\left(\theta-L_\theta\right)\right]\right\}\left\{1+\cos\left[\frac{\pi}{L_{\bar{z}}}\left(\bar{z}-L_{\bar{z}}\right)\right]\right\} \tag{4}$$

Surface roughness parameters are shown in the following fig.

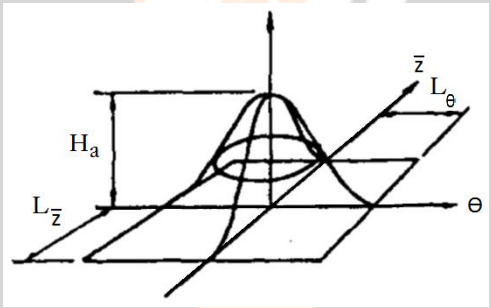

Fig 2: Three-dimensional Tsann asperity model [2]

Dimensionless pressure boundary conditions are shown in the following form

$$\bar{P}(0,\bar{z})=0,\bar{P}(0,\pm\Lambda)=0,$$
$$\bar{P}(\pi,\bar{z})=d\bar{P}/d\,\theta(\pi,\bar{z})=0 \tag{5}$$

By setting all negative pressures, the pressure of the leading edge boundaries, and the location of the starting of cavitation zone equal to zero, the Reynolds modified equation is established.
related your research work Introduction related your research work Introduction related your research work Introduction related your research work Introduction related your research work Introduction related your research work Introduction related your research work In

3. Bearing performance characteristics

With the pressure field known, the bearing performance calculations can be carried out. The dimensionless radial and tangential load components are found in the from

$$\begin{bmatrix}\bar{W}_x\\ \bar{W}_y\end{bmatrix}=-\int_0^1\int_0^{2\pi}\bar{P}_i\begin{bmatrix}\cos\theta\\ \sin\theta\end{bmatrix}d\theta d\bar{z} \tag{6}$$

The load capacity is written as

$$\bar{W} = \left(\bar{W}_x^2 + \bar{W}_y^2 \right)^{\frac{1}{2}} \tag{7}$$

Attitude angle is an angle from a fixed line connecting the center of the bearing with the center of the journal to a line, which is in the direction of the load vector. This angle is defined based on the idea that the input load is just supported in vertical direction and is calculated by an iterative method.
The angle is obtained as follows:

$$\phi_0 = \arctan\left(\frac{X_j}{Y_j} \right) = \arctan\left(\frac{\bar{W}_x}{\bar{W}_y} \right) \tag{8}$$

The dimensionless friction force is given by

$$\bar{F} = \sum_{i=1}^{1} \int_{-\lambda}^{\lambda} \int_{\theta_1^i}^{\theta_2^i} A \, d\theta \, d\bar{z} + \int_{-\lambda}^{\lambda} \int_{\theta_1^i}^{\theta_2^i} A \frac{\bar{h}\left(\theta_2^i\right)}{\bar{h}} \, d\theta \, d\bar{z} \tag{9}$$

Where

$$A = \frac{\bar{h}}{2} \frac{\partial \bar{p}}{\partial \theta} + \frac{1}{\bar{h} - \frac{2N}{l_m} \tanh\left(\frac{N l_m \bar{h}}{2} \right)} \tag{10}$$

Consequently, the friction coefficient is [9]

$$f\left(R/C\right) = \frac{\bar{F}}{\bar{W}} \tag{11}$$

The non-dimensional side leakage flow rate is [10]

$$\bar{Q} = 2 \int_0^{2\pi} \psi\left(N, \Lambda, h\right) \left(\frac{R}{L} \right)^2 \left. \frac{\partial \bar{p}}{\partial \bar{z}} \right|_{\bar{z}=0} d\theta \tag{12}$$

4. Numerical solution of equations

Approximating functions depend on the geometry and the number of nodes in each element. Needed algebraic functions for finding unknown coefficients will be derived by Reighley-Ritz and weighted residual methods after extracting the approximating functions.

Generally, the main finite element steps in analyzing a problem are as follows
1- Discretizing the domain area into elements include the numbering of nodes and elements, and, driving required geometric properties (such as coordinates, areas, etc).
2- Deriving the equations for every element:
a- Forming variation functions for the differential equation.

b- Considering $u = \sum_{j=1}^{n} c_j N_j$ as a dependent variable and substituting in the form of $\left[K^{(e)}\right] \times \left\{u^{(e)}\right\} = \left\{F^{(e)}\right\}$ in order to accessing element equations.
c- Deriving the interpolation functions and element matrices.
3- Combining element equations to obtain the general equation of the problem:
a- Creating a continuity between the elements in the primary variables.

b- Creating a balance between the elements in the secondary variables.
4- Applying boundary conditions.
5- Solving the combined equation.

Usually flow charts regarding applying numerical solution are exhibited as a schematic of the solution procedure and a way of achieving answer. The flow chart concerning this paper is as follows (fig 3):

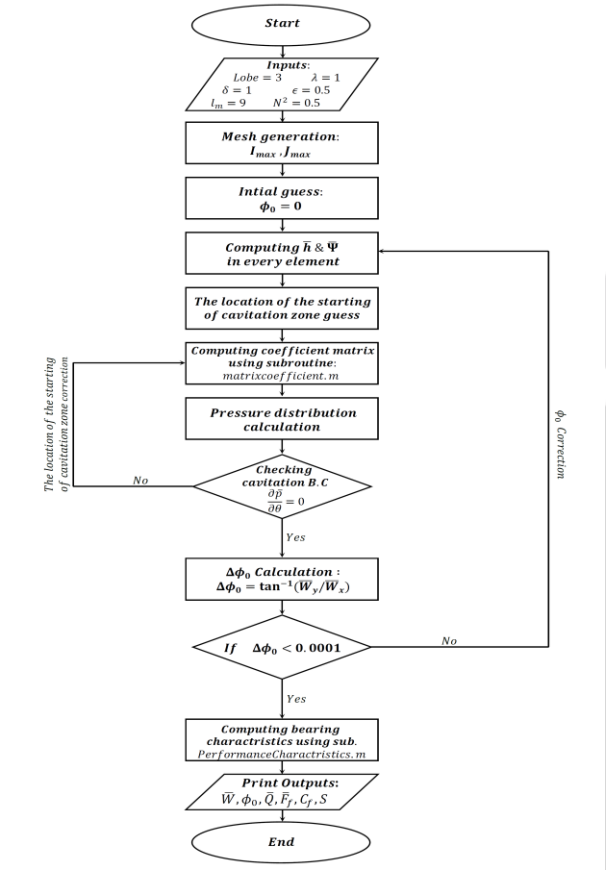

Fig 3: Numerical solution flow chart

5. Results and Discussion

Firstly, to prove the accuracy of the written numerical model, the dimensionless coefficient of friction as function of m, ε, and N^2 was compared with the published results [7] for two-lobe bearings.

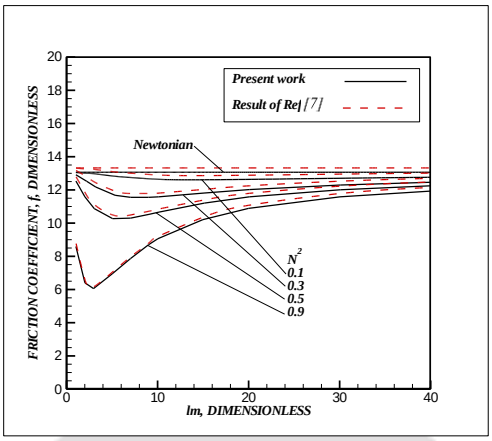

Fig 4: Dimensionless friction coefficient as a function of characteristic length for both Newtonian and micro-polar fluids in two-lobe bearings $(L/D=1, m=0.5, \dot{o}=0.5)$.

Fig 4 shows that there is a close agreement between the results and [7].

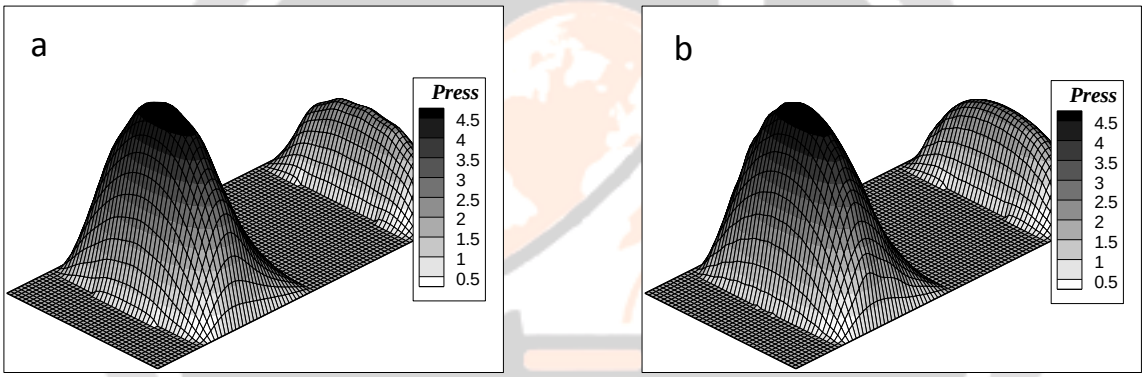

Fig 5: Pressure distribution for a micro-polar fluids with the asperity height of $(\bar{H}_a = 0.1)$ in two-lobe bearings when a) $L_o = \pi/5, L_z = 0.10$ b) $L_o = \pi/10, L_z = 0.05$ $(\lambda=1, m=0.5, \dot{o}=0.5, l_m=10, N^2=0.5)$.

There are two important parameters to determine the effects of micro-polar fluid lubrication on two-lobe loaded bearings. The first dimensionless parameter is the coupling number, which specifies coupling features of micro rotational fluid particles in linear and angular momentum equations. Higher values N^2 represent more strong effect between linear and angular equations. When the number approaches zero, the micro-polarity effect decreases and fluid is considered as Newtonian. The second dimensionless parameter is characteristic length, which describes the relationship between the bearing geometry and boundary layer thickness; moreover, it is a function of fluid molecular size. Lower values of this correspond larger characteristic length respect to the clearance and when it approaches infinity, a lubricant will be close to a Newtonian fluid.

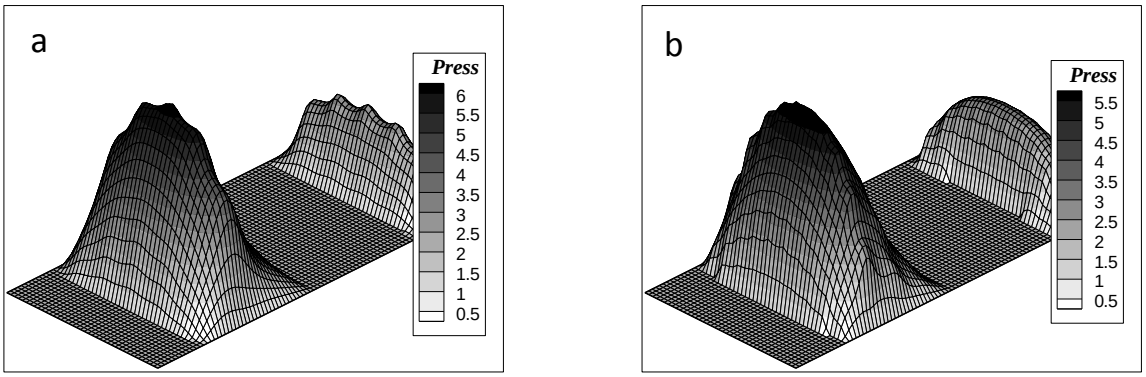

Fig 6: Pressure distribution for a micro-polar fluids with the asperity height of $(\overline{H}_a = 0.25)$ in two-lobe bearings when a) $L_\theta = \pi/5, L_{\overline{z}} = 0.10$ b) $L_\theta = \pi/10, L_{\overline{z}} = 0.05$ $(\lambda = 1, m = 0.5, \dot{o} = 0.5, l_m = 10, N^2 = 0.5)$.

Pressure distribution was obtained by solving modified Reynolds equation via numerical finite element program for micro-polar fluids with considering the Tsann roughness theory. It can be seen that the pressure distribution profiles are changed considerably when the roughness model is applied. The effect of the various parameters regarding Tsann roughness model on pressure distribution are shown in the figs. Comparing figs 5a to 6a and figs 5b to 6b depict that increasing the dimensionless height in Tsann model leads to increasing the pressure distribution profile and makes those teeth-shaped as well. As asperity length and width in a particular asperity height reduces, the peak of the pressure distribution decreases and become more uniformly (fig 5). Increasing the asperity height, this effect is more visible (fig 6).

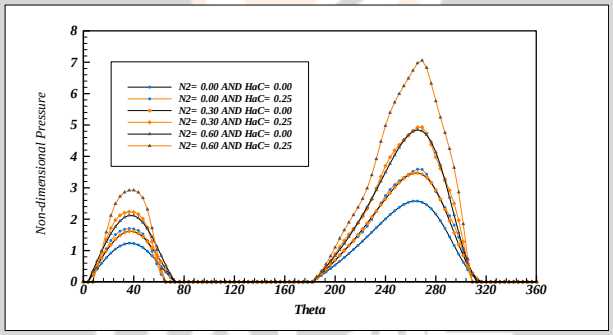

Fig 7: pressure distribution with considering Tsann theory for micro-polar fluids in the direction of the θ in the central line of two-lobe bearings $(L/D = 1, m = 0.5, l_m = 10, N^2 = 0.5)$.

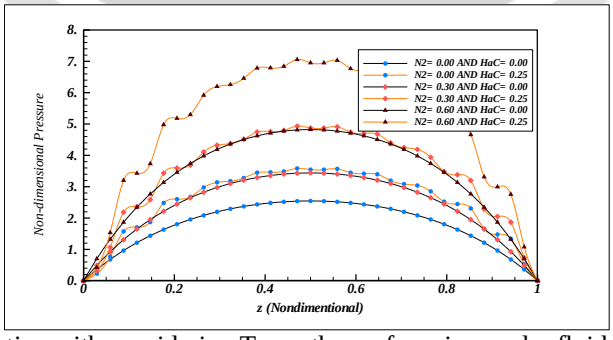

Fig 8: pressure distribution with considering Tsann theory for micro-polar fluids in the direction of the $\overline{z}\,(\theta = 3\pi/2)$ in the central line of two-lobe bearings $(L/D = 1, m = 0.5, l_m = 10, N^2 = 0.5)$

Figs 7 and 8 represent the pressure distribution, which were selected in the direction of the θ and z in the central line of the two-lobe bearings.

Generally, when the asperity height and the dimensionless coupling number are increased, the pressure distribution is increased as well.

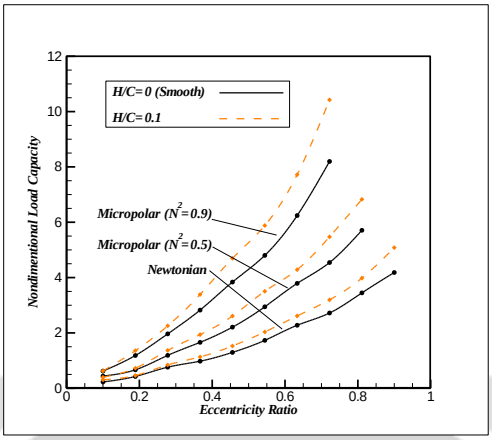

Fig 9: Dimensionless load capacity as a function of eccentricity ratio for both Newtonian and micro-polar fluids considering Tsann theory in two-lobe bearings $(L/D=1, m=0.5, l_m=9)$ **.**

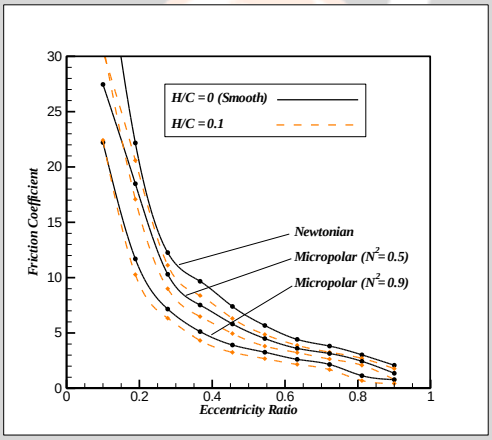

Fig 10: Dimensionless friction coefficient as a function of eccentricity ratio for both Newtonian and micro-polar fluids considering Tsann theory in two-lobe bearings $(L/D=1, m=0.5, l_m=9)$ **.**

All of the bearing performance parameters can be achieved after obtaining pressure distribution.

Figs 9 and 10 portray the bearing performance parameters changes in terms of eccentricity ratio in a particular characteristic length with respect to presence of Tsann roughness model. Graphs show when coupling number is increased in a particular eccentricity ratio the dimensionless load capacity is increased too (fig 9), although, dimensionless friction coefficient is decreased (fig 10).

Increasing eccentricity ratio with asperity height of 0.1 leads to increase the dimensionless load capacity for both Newtonian and micro-polar fluids (N^2 = 0.5 and N^2 = 0.9). This feature will intensify when micro-polarity properties are increased so that as the fluid become more non-Newtonian, the effect of increasing the asperity height is become more obvious regarding dimensionless load capacity term (fig 9) and there is a 6 percent deduction in dimensionless friction coefficient when eccentricity ratio is increased in the two lobe-bearings (fig 10).

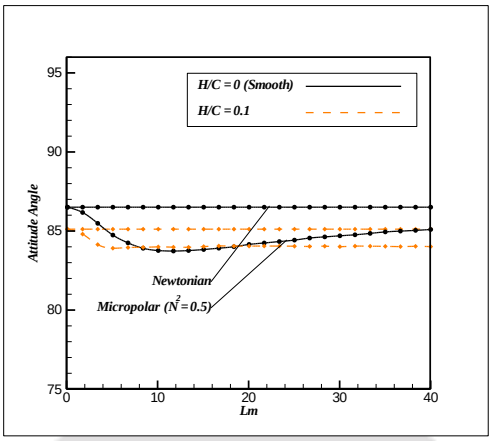

Fig 11: Attitude angle as a function of characteristic length for both Newtonian and micro-polar fluids considering the Tsann theory in two-lobe bearings $(L/D=1, m=0.5, \dot{o}=0.5)$.

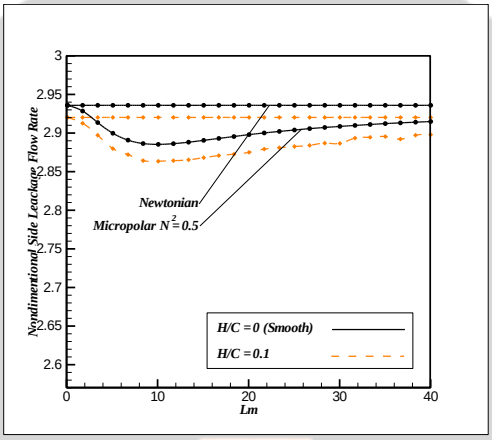

Fig 12: Attitude angle as a function of characteristic length for both Newtonian and micro-polar fluids considering the Tsann theory in two-lobe bearings $(L/D=1, m=0.5, \dot{o}=0.5)$.

Figs 11 and 12 show plots in conjunction with the bearing performance parameters in terms of increasing characteristic length from 0 to 40 for both Newtonian and non-Newtonian fluids in a particular eccentricity ratio. Reduction in side leakage flow rate and attitude angle are clear in the fig 11 and fig 12, respectively.

6. CONCLUSIONS

The main purpose of this study was to evaluate the effect of Tsann roughness model on micro-polar fluids in two-lobe bearings. Micro-polar fluids are a subset of micro fluids, which demonstrate micro rotation properties; this means that the fluid by having a microstructure is able to rotate independently on micro-volume without any change. Finite element method was used for solving dimensionless micro-polar fluids equation in the two-lobe bearing and the conclusions are as follows:

1- As the coupling number is increased, micro-polar fluid properties are become more prominent, moreover, the fluid viscosity is increased, and pressure distribution is intensified in particular asperity features.
2- Pressure distribution in mainly influenced by asperity profile height.
3- Increasing roughness parameters, especially asperity height, the teeth-shaped profile can be seen in pressure distribution.
4- Changing the width and the length of asperity profiles, pressure distribution does not vary regardless of whether fluid is Newtonian or micro-polar.
5- On a particular characteristic length, increasing eccentricity ratio, the peak of pressure distribution is increased and this feature can go further if Tsann roughness model is considered.

6- On a particular eccentricity ratio, increasing characteristic length, the peak of pressure distribution is decreased and this feature intensified if Tsann roughness model is considered.

7. List of Symbols

C	Bearing clearance, m
c_d, c_a	Angular viscosity coefficients, Ns/m^2
C_m	Minimum clearance when the center bearing and shaft are concentric, m
D	Lobe bearing diameter, m
$\bar{F}$	Dimensionless friction force
f	Dimensionless friction coefficient
$\bar{H}$	Dimensionless lubricant layer thickness
$\bar{H}_a$	Dimensionless asperity height
h	The lubricant layer thickness regardless of the Tsann roughness model, m
$\bar{h}$	Dimensionless lubricant layer thickness regardless of the roughness model, (h/C)
L	Bearing axial length, m
$L_{\bar{z}}$	Dimensionless half asperity width in z direction, m
L_θ	Dimensionless half asperity length in θ direction, m
l_m	Dimensionless micro-polar fluid characteristic length
m	Preload of the bearing, (C_m/C)
N	Coupling number, ($N= \mu_r / \mu + \mu_r)^{1/2}$
P	Hydrodynamic pressure, N / m2
$\bar{P}$	Dimensionless hydrodynamic pressure
$\bar{Q}$	Dimensionless side leakage flow rate
R	Shaft radius, m
$\bar{W}$	Dimensionless load capacity
$\bar{W}_x, \bar{W}_y$	Dimensionless load capacity components in x and y direction
x, y	Subtitles for components
z	Coordinate axis in axial direction, m
$\bar{z}$	Dimensionless axial length, *(z/L)*

Greek symbols

$\bar{\delta}$	Asperity profile, m
$\grave{o}$	Eccentricity ratio
θ	The angular coordinate measured from the x-axis
Λ	Dimensionless characteristic length
μ	Newtonian lubricant viscosity, Ns / m^2
μ_r	Partial rotational viscosity, Ns / m^2
φ_0	Attitude angle

8. REFERENCES

[1]. Turaga, R., Sekhar A., and Majumdar B., 1996, "Stochastic FEM model of one-dimensional hydrodynamic bearings with rough surfaces". Wear, p. 221-227.

[2]. Lin, T.-R., 1996, "Hydrodynamic lubrication of journal bearings including micropolar lubricants and three-dimensional irregularities". Wear, p. 21-28.

[3]. Prasad, E.S., Nagaraju, T., and Sagar, J.P, "Thermohydrodynamic Performance of a Journal Bearing with 3D-Surface Roughness and Fluid Inertia Effects".

[4]. Hsu, T, 2013, "Lubrication performance of short journal bearings considering the effects of surface roughness and magnetic field". Tribology International, p. 169-175.

[5]. Pinkus, O., 1956, "Analysis of elliptical bearings". Trans. ASME, p. 965-976.

[6]. Lund, J. and Thomsen, K, 1978, "A calculation method and data for the dynamic coefficients of oil-lubricated journal bearings". Topics in fluid film bearing and rotor bearing system design and optimization.

[7]. Rahmatabadi, A., Nekoeimehr, M., and Rashidi, R., 2010, "Micropolar lubricant effects on the performance of noncircular lobed bearings". Tribology International, p. 404-413.

[8]. Rahmatabadi, A., Zare Mehrjardi, M. and Fazel, M. 2010, "Performance analysis of micropolar lubricated journal bearings using GDQ method". Tribology International, p. 2000-2009.

[9]. Das S, Guha SK, Chattopadhyay AK. 2002, "On the steady-state performance of misaligned hydrodynamic journal bearing lubricated with micropolar fluids". Tribol Int ,p.201–10.

[10]. Wang XL, zhu KQ. 2004, "A study of the lubricating effectiveness of micropolar fluid in a dynamically loaded journal bearing". Tribol Int,p. 481–490.